Graphene Oxide/Nucleic Acid-Stabilized Silver Nanoclusters: Functional Hybrid Materials for Optical Aptamer Sensing and Multiplexed Analysis of Pathogenic DNAs

*Xiaoqing Liu, Fuan Wang, Ruth Aizen, Omer Yehezkeli, and Itamar Willner**

Institute of Chemistry, Center for Nanoscience and Nanotechnology, The Hebrew University of Jerusalem, Jerusalem 91904, Israel.

*Address correspondence to: willnea@vms.huji.ac.il

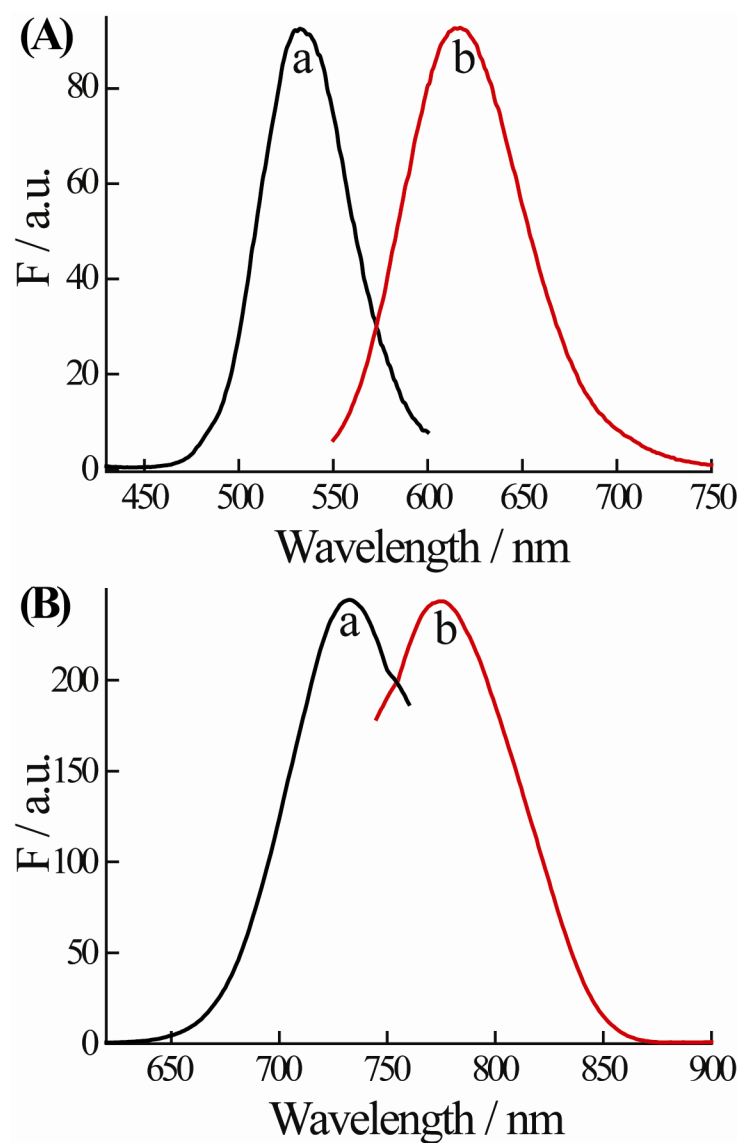Tel: +972-2-6585272

Fax: +972-2-6527715

Figure S1. Excitation (a) and emission (b) spectra corresponding to: (A) The red-emitting AgNCs stabilized by (**1**), and (B) The near infrared-emitting AgNCs stabilized by (**2**).

The elongation of the protecting nucleic acids (domain I) stabilizing the AgNCs with a foreign nucleic acid sequence (domain II) provides, however, an anchoring sequence that binds to GO, and the interaction of the elongated nucleic acid (**3**) that includes the AgNCs labels with GO, results in the adsorption of (**3**) to GO. Adsorption of (**3**) to GO leads to the effective quenching of the fluorescence of the AgNCs. This is exemplified in Figures S2, with the quenching of the (**3**)-modified AgNCs by GO. The binding of the (**3**)-functionalized AgNCs to GO, and their fluorescence quenching by GO, provides the principle for the application of the hybrid nanostructures for sensing, Figure S3(A). The interaction of the hybrid with a nucleic acid (**4**) that is complementary to the elongated domain II of (**3**), results in the formation of the duplex structure (**3**)/(**4**) that dissociated from GO, thus triggering on the luminescence of the AgNCs. Thus, the domain II of (**3**) acts as a probe for the target (**4**). For the marked domains see experimental section. Figure S3(B) depicts the time-dependent fluorescence changes upon challenging the (**3**)/GO hybrid with (**4**). The observed time-dependent increase implies that (**3**) is, indeed desorbed from the GO through the formation of the (**3**)/(**4**) duplex structure. Control experiment revealed that in the absence of GO, the addition of the nucleic acid, (**4**) to (**3**) does not lead to fluorescence changes of the AgNCs. Also, treatment of the (**3**)-functionalized GO with a foreign nucleic acid (**5**), that is not complementary to domain II of (**3**), does not lead to any fluorescence changes of the AgNCs. These results imply that the generation of the fluorescence originates only upon the formation of the (**3**)/(**4**) duplex that is desorbed from GO. Figure S3(C) shows the fluorescence spectra resulting in upon the interaction of the (**3**)-AgNCs/GO hybrid with different concentrations of (**4**) for a fixed time-interval of 80 min. As the concentration of the complementary nucleic acid (**4**) increases, the luminescence intensities of the released red-emitting AgNCs-labeled probe (**3**) are intensified. The target DNA, (**4**), could be analyzed with a detection limit of 1 nM. A further aspect to consider relates to the selectivity of the sensing platform and its ability to discriminate base mutations. Figure S3(C), inset, shows the fluorescence intensities upon analyzing (**4**), curve (a), by the AgNCs-(**3**)-modified GO, in comparison to the analysis of the one-base mismatch sequence (**4a**), curve (b). The desorption of the

fluorescence probe (**3**)-AgNCs from GO is less efficient in the presence of (**4a**), implying that a single-base mutation can be easily discriminated from the target DNA.
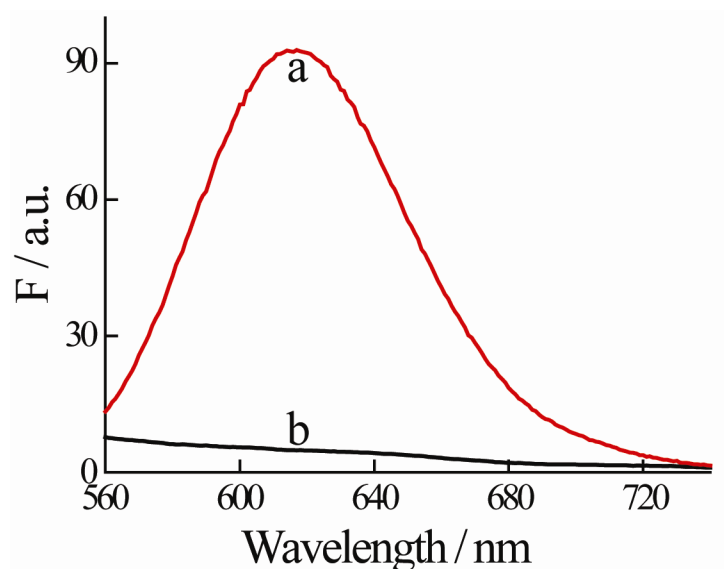

Figure S2. Fluorescence spectra of the red-emitting AgNCs stabilized by (**3**) in the absence (a) and presence (b) of GO.
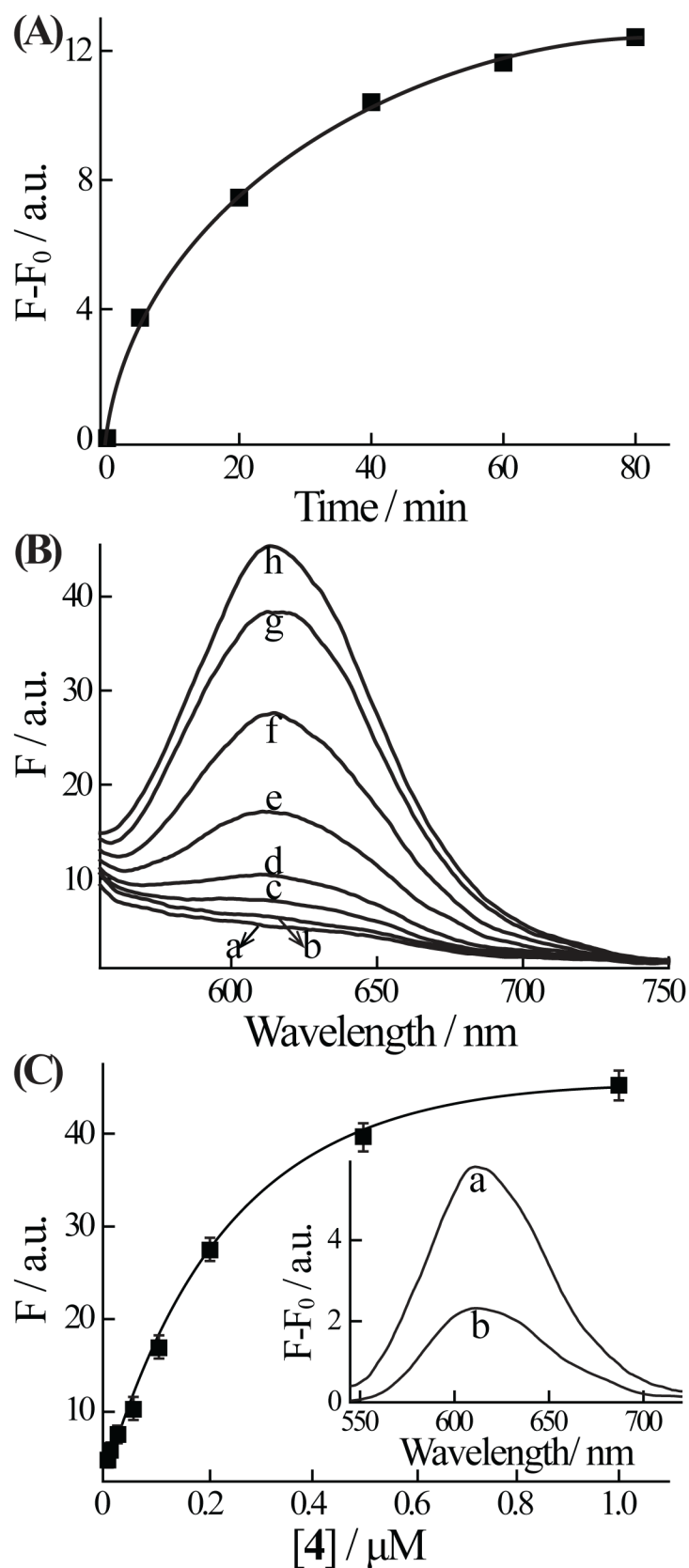
Figure S3. (A) Time-dependent fluorescence changes of the red-emitting AgNCs at λ = 616 nm upon

addition of 100 nM (**4**) to the (**3**)-AgNCs/GO hybrid. (B) Fluorescence spectra of the (**4**)/(**3**)-AgNCs

released form GO upon analyzing different concentrations of target DNA (**4**) by the (**3**)-AgNCs/GO system: (a) 0, (b) 5 nM, (c)20 nM, (d) 50 nM, (e)100 nM, (f) 200 nM, (g) 500 nM, and (h) 1000 nM. Fluorescence spectra were recorded after a fixed time-interval of 80 min. (C) Calibration curve corresponding to the luminescence signal at λ=616 nm. Inset: Fluorescence spectra corresponding to the analysis of: (a) The fully complementary target (**4**), 50 nM and (b) the one-base mismatched nucleic acid (**4a**), 50 nM, by the (**3**)-AgNCs/GO matrix. F_0 and F correspond to the fluorescence of the system in the absence and presence of target DNA, respectively.
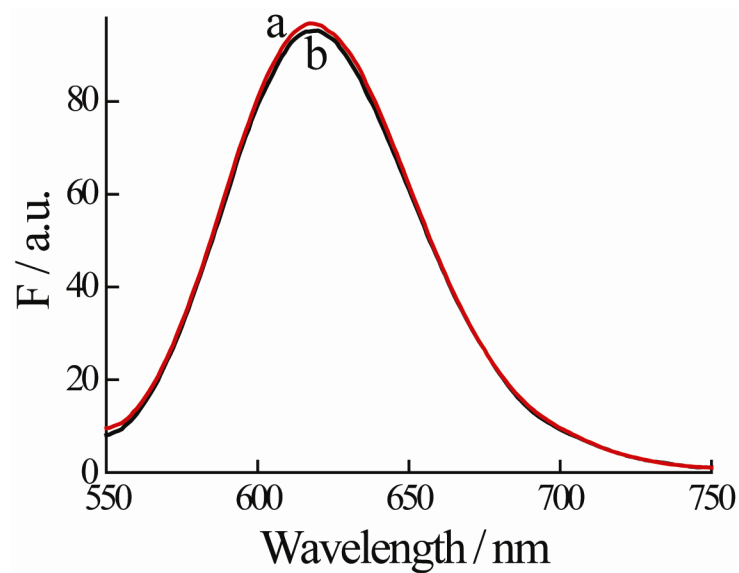
Figure S4. Fluorescence spectra of the AgNCs stabilized by the probe (**6**) before (a) and after (b) addition of HBV target gene (**5**), in the absence of GO.
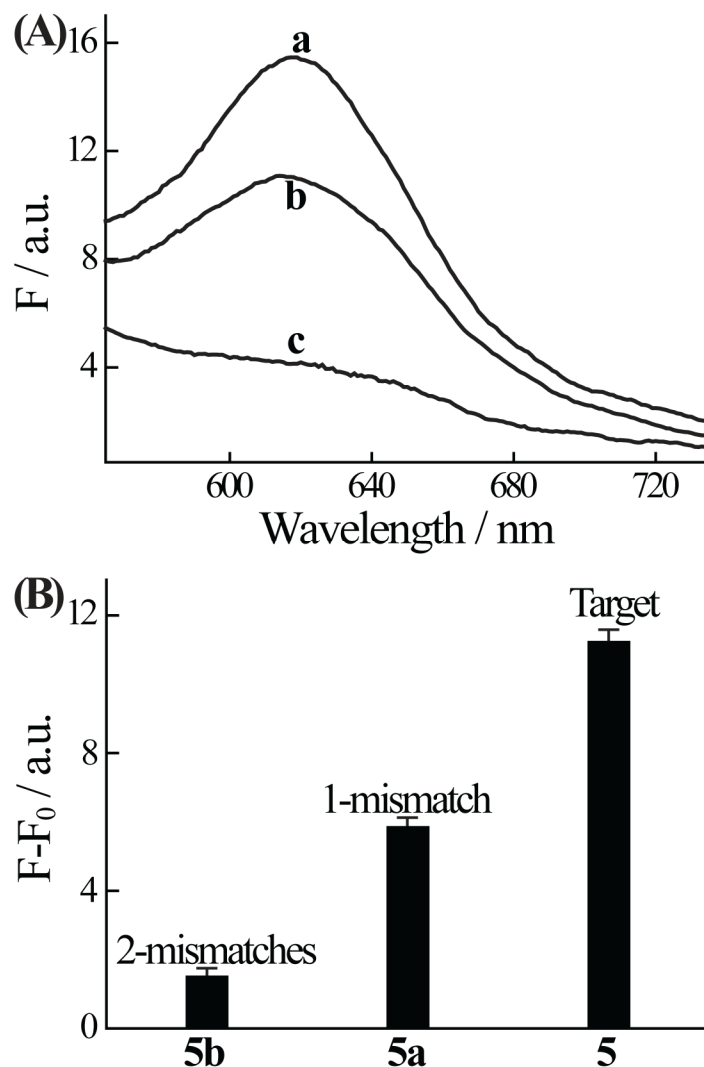
Figure S5. Fluorescence spectra (A) and corresponding intensity changes (B) resulting in upon the challenging of the (**6**)-AgNCs/GO with the HBV target gene (**5**), one-base mutant gene (**5a**), and two-base mutant gene (**5b**), each 50 nM, $\lambda = 616$ nm. Fluorescence spectra were recorded after a fixed time-interval of interaction corresponding to 80 min. F_0 and F correspond to the fluorescence of the system in the absence and presence of target DNA, respectively.

The ability to distinguish between the HBV target (**5**) and its single base mutant (**5a**) was further examined under stringency control by following the effect of ionic strength or temperature on the luminescence yields of the desorbed duplex DNA structures. Examination of these parameters on the resulting fluorescence by the target or mutant is particularly important since these parameters might not control only the stability of the resulting duplexes, but may affect also the desorption efficiencies from

the GO. Figure S5(A), curve (a), shows the fluorescence spectrum generated by the target DNA (**5**), upon desorption of the AgNCs (**6**)/(**5**) duplex from the GO (maximum fluorescence intensity, F_T). Figure S5(A), curve (b) depicts the fluorescence spectrum of the AgNCs upon removal of the mutant in the form of the duplex (**6**)/(**5a**) from the GO (maximum fluorescence intensity, F_M). Figure S5(A), curve (c), shows the fluorescence spectrum of the system in the absence of any target and it corresponds to the background signal of desorbed AgNCs (maximum fluorescence marked F_0). These spectra were recorded in the presence of (**5**) or (**5a**), 50 nM, ionic strength 200 mM at room temperature 25˚C. Accordingly, we examined the ability to distinguish between the HBV (**5**) target and its single-base mismatch (**5a**) under stringency control by temperature/ionic strength. The differentiation parameter between (**5**) and (**5a**) was defined as $(F_T - F_0)/(F_M - F_0)$. That is the higher value of the "differentiation parameter", the better discrimination between the target and mutant will be achieved.

Table S1(A) shows the effect of temperature on the "differentiation parameter". As the temperature increases the "differentiation parameter" is higher. This result is consistent with the fact that the duplex structure between (**6**)/(**5a**) is weaker as temperature increases (lower melting temperature). Thus, the desorption of (**6**)/(**5**) is more efficient than the desorption of (**6**)/(**5a**) at higher temperature.

The effect of ionic strength on the "differentiation parameter" is shown in Table S1(B). As the ionic strength is higher the "differentiation parameter" increases. This is mainly attributed to the higher binding affinity of the Ag NCs-modified probes to GO at higher ionic strength (at low ionic strength the probes are significantly desorbed from GO as single strands). Thus the energetically less stabilized duplexes between the Ag NCs (**6**)/(**5a**) lead to inefficient desorption of the probes form GO, yielding high "differentiation parameters".

Table S1(A)

Temperature / $^\circ$C	$(F_T-F_0)/(F_M-F_0)$
15	1.53
25	1.60
35	1.72
45	1.90

Table S1(B)

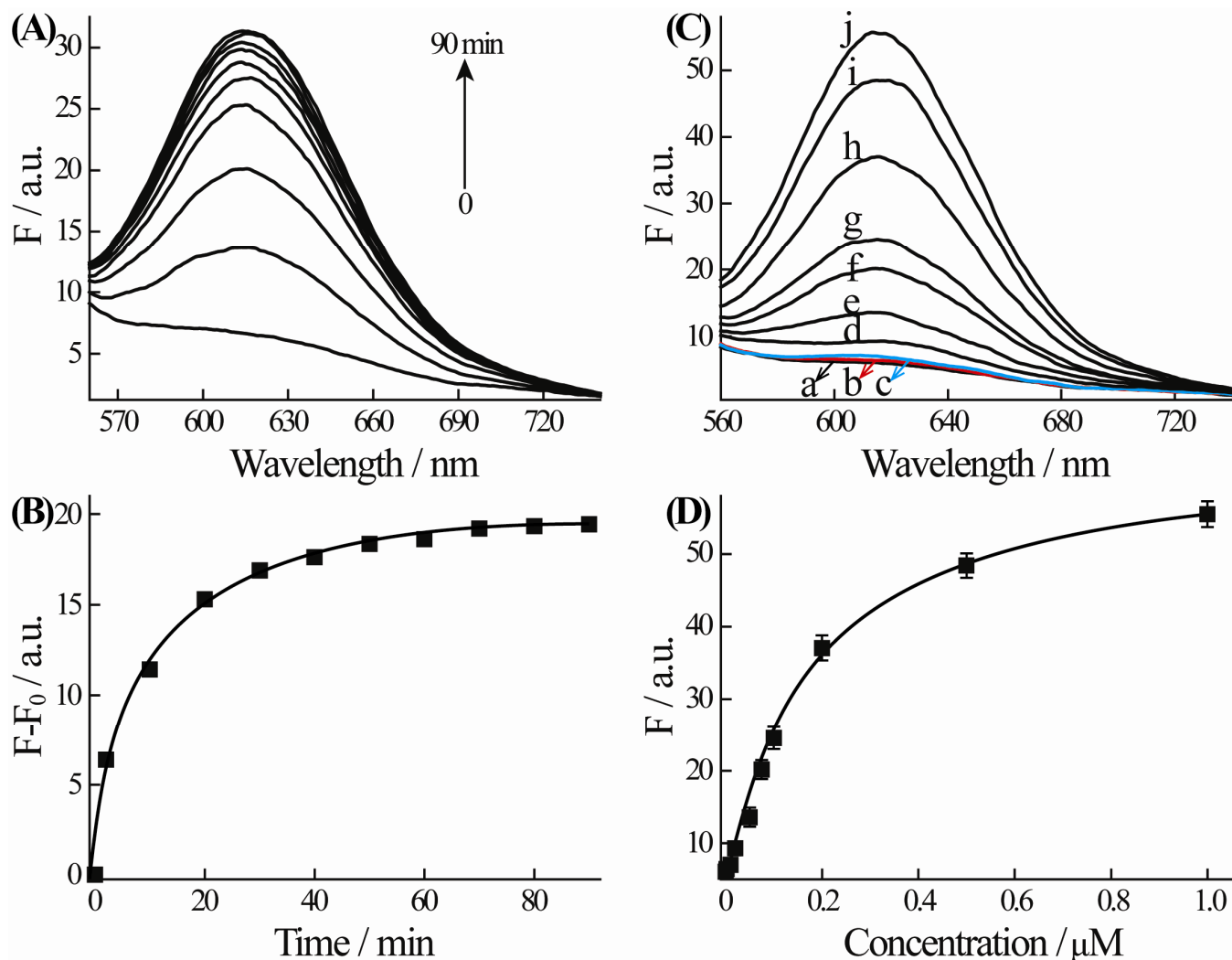| Salt concentration/mM	$(F_T-F_0)/(F_M-F_0)$
120	1. 22
200	1. 65
280	2. 01

Figure S6. (A) Time-dependent fluorescence spectra of the red-emitting AgNCs upon addition of 100 nM of HIV gene (**8**) to the (**7**)-AgNCs/GO hybrid. (B) Time-dependent fluorescence changes at λ=616 nm upon analyzing 100 nM (**8**) by (**7**)-AgNCs/GO. F_0 and F correspond to the fluorescence of the system in the absence and presence of target DNA, respectively. (C) Fluorescence spectra of the AgNCs upon analyzing different concentrations of HIV gene (**8**) by the (**7**)-AgNCs/GO system: (a) 0, (b) 2 nM, (c)10 nM, (d) 20 nM, (e) 50 nM, (f) 75 nM, (g) 100 nM, (h) 200 nM, (i) 500 nM, and (j)1000 nM. Fluorescence spectra were recorded after a fixed time-interval of 80 min. (D) Calibration curve corresponding to the luminescence signal at λ=616 nm. Error bars were derived from N=3 experiments.
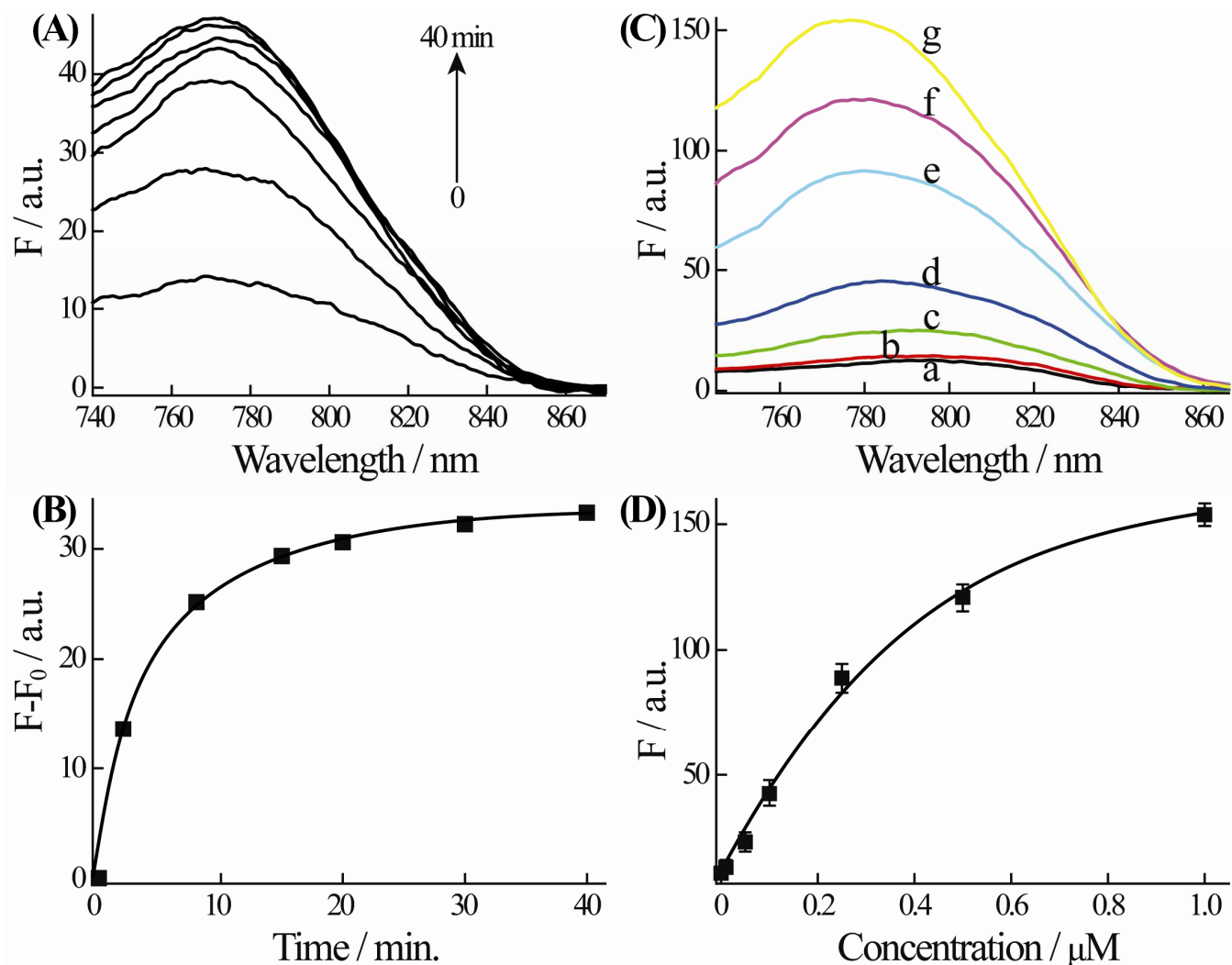
Figure S7. (A) Time-dependent fluorescence spectra of the near infrared-emitting AgNCs upon addition of 100 nM of HBV gene (**5**) to the (**10**)-AgNCs/GO hybrid. (B) Time-dependent fluorescence changes of the near infrared-emitting AgNCs at λ=775 nm upon analyzing 100 nM (**5**) by (**10**)-AgNCs/GO. F_0 and F correspond to the fluorescence of the system in the absence and presence of target DNA, respectively. (C) Fluorescence spectra of the AgNCs upon analyzing different concentrations of HBV gene (**5**) by the (**10**)-AgNCs /GO system: (a) 0, (b) 10 nM, (c) 50 nM, (d) 100 nM, (e) 250 nM, (f) 500 nM, and (g) 1000 nM. Fluorescence spectra were recorded after a fixed time-interval of 60 min. (D) Calibration curve corresponding to the luminescence signal at λ=775 nm. Error bars were derived from N=3 experiments.
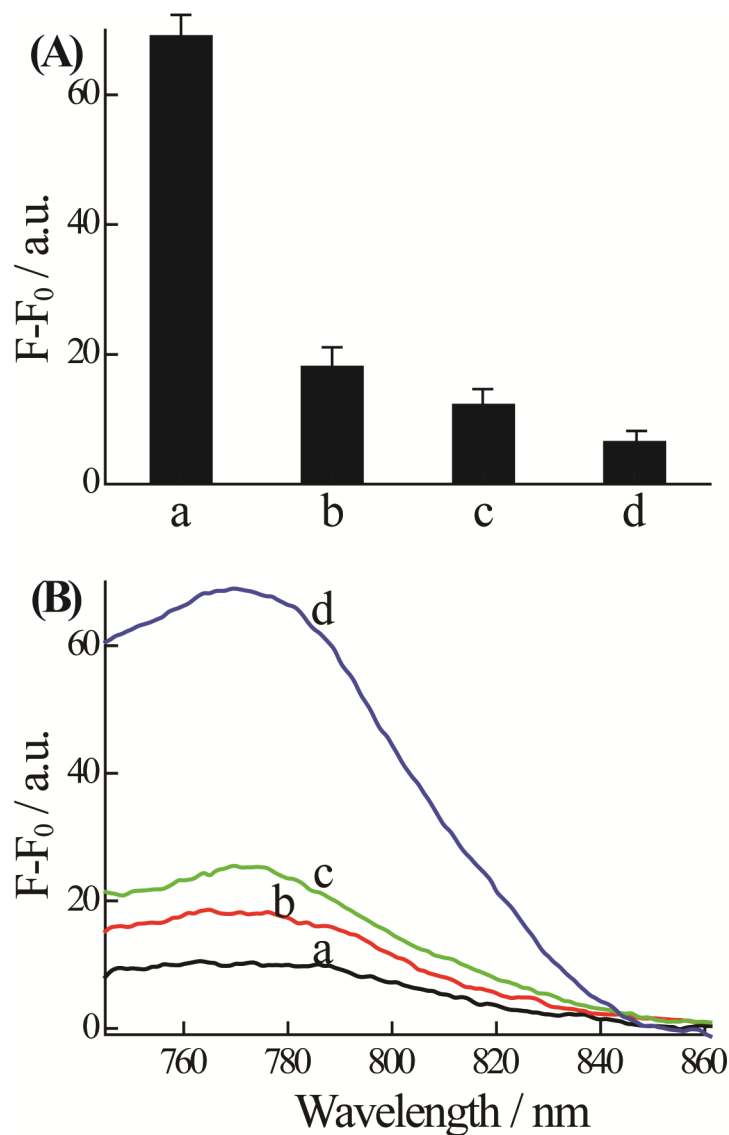
Figure S8. (A) Fluorescence intensity changes ($\lambda=775$ nm) of near infrared-emitting AgNCs upon addition of 200 nM of HIV gene (**8**) to the (**9**)-AgNCs/GO system. The AgNCs were synthesized using different molar ratio of DNA (**9**)-AgNO$_3$-NaBH$_4$: (a) 1:6:6, (b) 1:8:8, (c) 1:8:4, (d) 1:16:8. Fluorescence spectra were recorded after a fixed time-interval of 60 min. F_0 and F correspond to the fluorescence of the system in the absence and presence of target DNA, respectively. (B) Fluorescence spectra changes of near infrared-emitting AgNCs upon addition of 200 nM of HBV gene (**5**) to the (**10**)-AgNCs/GO system. The AgNCs were synthesized using different molar ratio of DNA (**10**)-AgNO$_3$-NaBH$_4$: (a) 1:6:6, (b) 1:8:8, (c) 1:8:4, (d) 1:16:8. Fluorescence spectra were recorded after a fixed time-interval of 60 min. F_0 and F correspond to the fluorescence of the system in the absence and presence of target DNA, respectively.
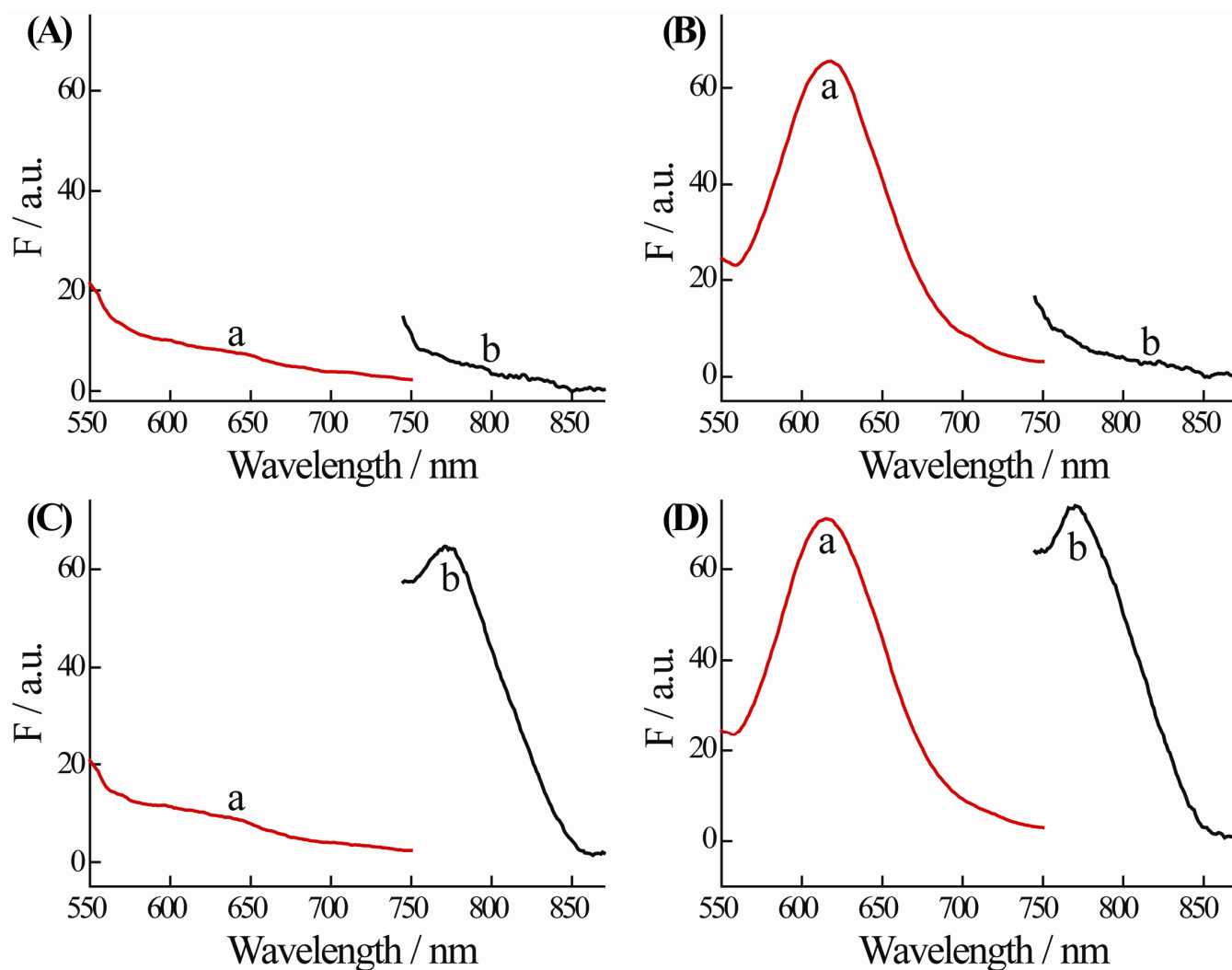
Figure S9. Fluorescence spectra of the AgNCs protected by probes (**10**) and (**12**): (A) In the absence of the gene targets. (B) In the presence of syphilis gene (**11**), and in the absence of HBV gene (**5**). (C) In the presence of HBV gene (**5**), and in the absence of syphilis gene (**11**). (D) In the presence of syphilis gene (**11**) and HBV gene (**5**). Curves (a) and (b) correspond to fluorescence of the red-emitting and the near infrared-emitting AgNCs, respectively.
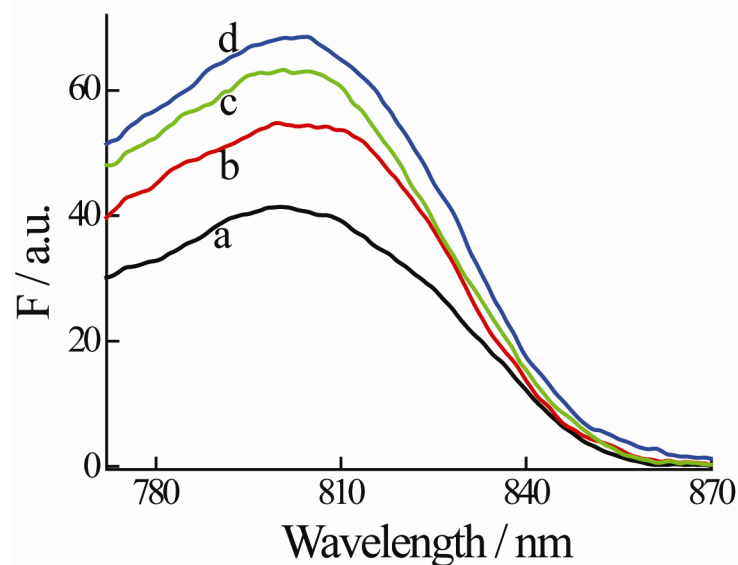
Figure S10. (A) Fluorescence spectra of the near infrared-emitting AgNCs upon analyzing different concentrations of ATP by the (**14**)-AgNCs/GO system: (a) 0, (b) 0.5 mM, (c) 1 mM, and (d) 1.5 mM.
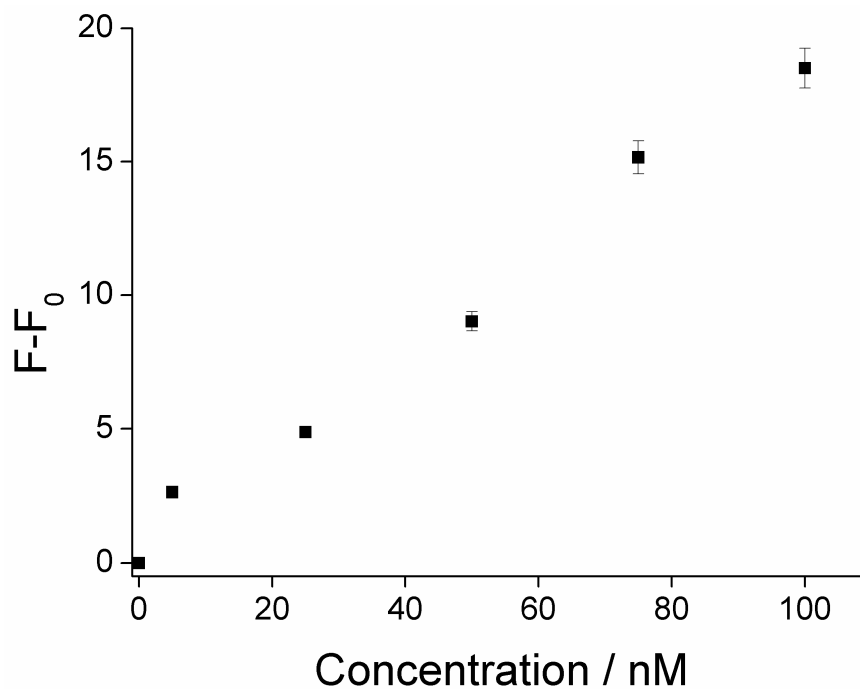

Figure S11. Calibration curve corresponding to the luminescence signal shown is Figure 5B.

Table S2. Optical DNA and aptamer-substrate sensing platforms

Method/System	Detection limit (nM)	Detection time-interval/h	Reference
DNA			
Fluorescence, GO/molecular beacon	2	2	13a
Fluorescence, Releasing acridine orange from reduced GO	50	-	13c
Fluorescence, Exo III-assisted target recycling	0.005	1.5	15*
Fluorescence, Autonomous DNAzyme machine	0.01	2.5-3	20a*
Fluorescence, Polymerization/nicking DNA machine	1-10	4-10	20b*
ISFET, Nucleic acid modified GO matrices	25	1-2	23
Chemiluminescence, G-Quadruplex DNAzyme	1	15	24
Colorimetric, G-Quadruplex DNAzyme	5.4	1	25
Fluorescence, GO/nucleic acid-stabilized AgNCs	0.5	1-1.5	Present study
ATP			
Fluorescence, Quenching of released dye from dsDNA by GO	0.45-3	2	21a
Colorimetric, G-quadruplex DNAzyme	1-10	3	21b
Fluorescence, Exo III-assisted analyte recycling	0.25	1-1.5	21c*
Fluorescence, Aptazyme-coupled rolling circle amplification	1	-	21d*
Fluorescence, Aptamer duplex/ethidium bromide/tetrahedralfluorene complex	20	–	26
Fluorescence, GO/nucleic acid stabilized AgNCs	2.5	1	Present study
Thrombin			
Colorimetric, G-quadruplex DNAzyme	20	5	22a
Fluorescence, Exo III-assisted analyte recycling	0.09	1-1.5	21c*
Fluorescence, Polymerization/nicking DNA machine	62.5	2	22b*
ISFET, Nucleic acid-modified GO matrices	25	1-2	23
Absorbance, Aptamer-functionalized Au nanoparticles	2	3	27
Bioluminescence, Sandwich-type immunoassay	10	1	28
Electrochemistry, Intercalation of MB in beacon aptamer	11	0.5	29
Electrochemical impedance spectroscopy, Disposable screen-printed electrodes modified with functionalized graphene	10–50	1	30
Fluorescence, GO/nucleic acid stabilized AgNCs	0.5	0.5-1	Present study

∗: amplified detection

Reference:

23. Sharon, E.; Liu, X.; Freeman, R.; Yehezkeli, O.; Willner, I. *Electroanalysis* **2012**, *25*, 851-856.

24. Pavlov, V.; Xiao, Y.; Gill, R.; Dishon, A.; Kotler, M.; Willner, I. *Anal. Chem.* **2004**, *76*, 2152−2156.

25. Zhang, L.; Zhu, J.; Li, T.; Wang, E. *Anal. Chem.* **2011**, *83*, 871−8876.

26. Wang, Y.; Liu, B. *Analyst*, **2008**, *133*, 1593-1598

27. Pavlov, V.; Xiao, Y.; Shlyahovsky, B.; Willner, I. *J. Am. Chem. Soc.* **2004,** *126*, 11768-11769.

28. Akter, F.; Mie, M.; Kobatake, E. *Analyst* **2012**, *137*, 5297-5301

29. Bang, G. S.; Cho, S. Kim, B. G. *Biosens. Bioelectron.* **2005**, *21*, 863-870.

30. Loo, A. H.; Bonanni, A.; Pumera, M. *Nanoscale* **2012**, *4*, 143-147.